The International Journal of Engineering and Science (IJES)
|| Volume || 7 || Issue || 5 Ver. III || Pages || PP 35-46 || 2018 ||
ISSN (e): 2319 – 1813 ISSN (p): 23-19 – 1805

Development of Composite Laminated Faceted Shells Using a Higher Order Finite Strip Element

Rizal Zahari, Seriampalayam Ramaswamy Ravishankar, Andrew Ordys
Systems Engineering Department, Military Technological College,
Muscat, Sultanate of Oman
Corresponding Author: Rizal Zahari

----------ABSTRACT----------
In the present study, a finite strip method for geometric non-linear static analysis based on the tangential stiffness matrix has been developed using the new concept of polynomial finite strip elements, with Reissner (higher order shear deformable element) plate-bending theory for composite faceted shells. A finite strip analysis programming package which is capable of performing non-linear analysis for composite folded plates has also been developed with Reissner plate bending element. Good agreement with the finite element analysis (ABAQUS) results has been observed through various test cases, confirming the accuracy and reliability of the new developed finite strip method.
KEYWORDS - *Finite strip method, Reissner plate bending theory, faceted shell, non-linear static analysis.*

Date of Submission: 16-05-2018 Date of acceptance: 31-05-2018

I INTRODUCTION

The finite strip method (FSM) can be regarded generally as a specialization of the finite element method (FEM). The properties of a strip are based on the use of an assumed displacement field in conjunction with the potential energy or virtual work principles. The first publication on the FSM was by Cheung [2], which concerned only the linear static analysis of single rectangular plates having a pair of opposite ends that were simply supported. Kermanidis and Labeas [3] developed an anisotropic finite strip element based on the semi-analytical method, for static and stability analysis of thin composite laminates. Wang et al. [4] investigated the critical buckling load of composite laminated plates using a developed higher order shear deformable plate finite strip element. The warping of cross-section and transverse shear deformation can be predicted by the higher order plate theories. Akhras et al. [5] have developed a new finite strip method for the large deflection analysis of composite laminates. The method incorporates additional degrees of freedom for each nodal line and uses the higher order shear deformation theory. Loughlan [6] employed semi-analytical finite strip method to investigate the effect of bend-twist coupling on a square anti-symmetric angle-ply laminated plate under compressive buckling.

In this work, the finite strip analysis of composite laminated facetted shells, which is based on a new derivation of the higher order shear element (Reissner type element [7], is presented taking into account the geometric non-linearity. This derivation follows concepts similar to those employed in the finite element analysis using the tangential stiffness matrix approach. The formulation of the finite strip equations are based on a new Reissner-*type* finite strip element [1] in which one-dimensional *Lagrangian* interpolation employed along both the length and the width of the plate. One the other hand, *Hermitian* interpolation is employed for the lateral deflection components together with appropriate reduced integration schemes. In this research, a new rotation matrix based on seven degrees of freedom per node has been derived for the facetted shell finite strip element.

II DERIVATIONS OF FINITE STRIP EQUATIONS

Displacement and strain components

Consider a composite laminated plate which is parallel to the x-y plane. The upper and lower surfaces of the plate are defined by $z = h/2$ and $z = - h/2$ respectively, where h is the thickness of the plate Based on Reissner's theory [7] the transverse shear strains at any point (x, y ,z) inside a plate can be represented by parabolic distributions across the thickness of the plate as follows:

$$\underline{\gamma}(x, y, z) = \begin{bmatrix} \gamma_{xz} \\ \gamma_{yz} \end{bmatrix} = \frac{3}{2}\begin{bmatrix} 1 - \frac{4z^2}{h^2} \end{bmatrix}\begin{bmatrix} \bar{\gamma}_{xz} \\ \bar{\gamma}_{yz} \end{bmatrix} \quad (1)$$

where $\bar{\gamma}_{xz}$ and $\bar{\gamma}_{yz}$ are the average values of the transverse shear strains over plate thickness.

From *Mindlin's* plate bending theory [8], the average slope angles are defined as follows:

$$\theta_x = \frac{\partial w}{\partial y} - \bar{\gamma}_{yz} \equiv \frac{\partial w}{\partial y} - \psi_x \qquad (2)$$

$$\theta_y = -\frac{\partial w}{\partial x} + \bar{\gamma}_{xz} \equiv -\frac{\partial w}{\partial x} - \psi_y \qquad (3)$$

Where $\psi_x = \bar{\gamma}_{yz}$, $\psi_y = -\bar{\gamma}_{xz}$

The average values of the transverse shear can be used to define the displacement components, which leads to

$$u(x, y, z) = u^{\circ}(x, y) - z\frac{\partial w}{\partial x} - \psi_y\left(\frac{3}{2}z - \frac{2z^3}{h^2}\right) \qquad (4)$$

$$v(x, y, z) = v^{\circ}(x, y) - z\frac{\partial w}{\partial y} + \psi_x\left(\frac{3}{2}z - \frac{2z^3}{h^2}\right) \qquad (5)$$

$$w(x, y, z) \approx w(x, y) \qquad (6)$$

Equations (4), (5), and (6) represent the displacement components at any point (*x, y, z*) inside the plate, where u°, v° represent the values of *u, v* at the mid-plane $z = 0$.

In this work the transverse shear strains are always assumed infinitesimal while for non-linear static analysis, the x-y strain components are assumed finite. Using Green's strain displacement equations [10], the strain tensor at any point inside the plate can be obtained using appropriate engineering notations [11].

Interpolated Displacement Equations

The interpolation of the lateral displacement w both in the x and y-directions requires the C^1 continuity [9]. In order to maintain C^1 continuity over the whole plate, only *Hermitian*-type can be used. All other displacement components are interpolated in the x and y-directions by means of *Lagrangian* interpolation, as there is no need for more than C° continuity required. Hence, **t**he full x-y interpolated displacement equations can be expressed for an n-node finite strip, with *m y*-terms (harmonics) as follows [1]:

$$u^{\circ}(x, y) = \sum_{r=1}^{m}\sum_{i=1}^{n} N_i(\xi)\mu_r(\eta)u_i^r \qquad (7)$$

$$v^{\circ}(x, y) = \sum_{r=1}^{m}\sum_{i=1}^{n} N_i(\xi)\mu_r(\eta)v_i^r \qquad (8)$$

$$\psi_x(x, y) = \sum_{r=1}^{m}\sum_{i=1}^{n} N_i(\xi)\mu_r(\eta)(\psi_x^r)_i \qquad (9)$$

$$\psi_y(x, y) = \sum_{r=1}^{m}\sum_{i=1}^{n} N_i(\xi)\mu_r(\eta)(\psi_y^r)_i \qquad (10)$$

$$w(x, y) = \sum_{r=1}^{m}\sum_{i=1}^{n} S_r(\eta)\left[G_i(\xi)w_i^r + H_i(\xi)w_{i,x}^r\right] \qquad (11)$$

where the shape functions $N_r(\zeta)$ and $\mu_r(\eta)$ are

$$N_i(\xi) = \prod_{\substack{j=1 \\ j \neq i}}^{n} \frac{(n-1)\xi - (j-1)}{i-j} \qquad (12)$$

$$\mu_r(\eta) = \prod_{\substack{s=1 \\ s \neq r}}^{m} \frac{(m-1)\eta - (s-1)}{r-s} \qquad (13)$$

which represent one dimensional *Lagrangian* shape functions and

$w_{i,x} = \left.\frac{\partial w}{\partial x}\right|_{at\ x=x_i} \equiv J_x w_{i,\xi}$ where

$\frac{dx}{d\xi} = a \equiv J_x, \quad \frac{dy}{d\eta} = b \equiv J_y$

and

$G_i(\xi) = g_i(\xi), \quad H_i(\xi) = J_x h_i(\xi)$

where

$$g_i(\xi) = [1 - 2\alpha_i(\xi - \xi_i)]\left[L_i^n(\xi)\right]^2$$

$$h_i(\xi) = (\xi - \xi_i)\left[L_i^n(\xi)\right]^2$$

$$\alpha_i = \sum_{\substack{r=1 \\ r \neq i}}^{n} \frac{1}{\xi_i - \xi_r}$$

$$L_i^n(\xi) = \prod_{\substack{r=1 \\ r \neq i}}^{n} \frac{(n-1)\xi - (r-1)}{i-r}$$

$m = 2m'$

$s =$ Integer of $\left(\frac{r+1}{2}\right)$

$S_r(\eta) \equiv G_s(m', \eta)$ for $r = 1,3,5$ .....

$S_r(\eta) \equiv H_s(m', \eta)$ for $r = 2,4,6$ .....

where $m = 2m'$

$s =$ Integer of $\left(\frac{r+1}{2}\right)$

which represent the hermitian interpolation in x and y where ξ, η are non-dimensional representation of *x*, *y* coordinates of the midplane.

Stress Components

The stress components at a point in the l^{th} layer, can also be partitioned and represented by the following vectors [1]:

$$\underline{\sigma}^{(l)} = \begin{bmatrix} \sigma_x \\ \\ \sigma_y \\ \\ \tau_{xy} \end{bmatrix} \qquad \underline{\tau}^{(l)} = \begin{bmatrix} \tau_{xz} \\ \\ \tau_{yz} \end{bmatrix} \tag{14}$$

Using stress-strain relations for the l^{th} layer, then:

$$\underline{\sigma}^{(l)} = \underline{D}^{(l)} \underline{\varepsilon} \tag{15}$$

$$\underline{\tau}^{(l)} = \underline{\mu}^{(l)} \underline{\gamma} \tag{16}$$

where $\underline{D}^{(l)}$, $\underline{\mu}^{(l)}$ are material stiffness matrices with respect to plate axes, for the l^{th} layer.

III DERIVATION OF ELEMENT STIFFNESS MATRICES

Using the principle of virtual work, the work done by actual loads is equal to the work done by equivalent nodal loading [8], i.e.:

$$d\chi = dU - dW = 0 \tag{17}$$

We then arrived at the following linearized non-linear equations [10] which are defined as:

$$\sum_{strips} \sum_{r=1}^{m} \left[\left(\underline{K}^{sr} + \underline{K}_{\sigma}^{sr} \right) \right] \Delta \underline{\delta}_o^r = \underline{R}^s \text{, for } s = 1,2, \ldots\ldots, m \tag{18}$$

where $\underline{K}^{sr}$ and $\underline{K}_{\sigma}^{sr}$ are the tangential and non-linear stiffness matrices respectively which can be partitioned for a strip as follows :

$$\underline{K}^{sr} = \begin{bmatrix} \underline{K}_{oo}^{sr} & \underline{K}_{ob}^{sr} & \underline{K}_{o\psi}^{sr} \\ \underline{K}_{bo}^{sr} & \underline{K}_{bb}^{sr} & \underline{K}_{b\psi}^{sr} \\ \underline{K}_{\psi o}^{sr} & \underline{K}_{\psi b}^{sr} & \underline{K}_{\psi\psi}^{sr} \end{bmatrix} \tag{19}$$

and

$$\underline{K}_{\sigma}^{sr} = \begin{bmatrix} \underline{K}_{\sigma\ oo}^{sr} & \underline{K}_{\sigma\ ob}^{sr} & \underline{K}_{\sigma\ o\psi}^{sr} \\ \underline{K}_{\sigma\ bo}^{sr} & \underline{K}_{\sigma\ bb}^{sr} & \underline{K}_{\sigma\ b\psi}^{sr} \\ \underline{K}_{\sigma\ \psi o}^{sr} & \underline{K}_{\sigma\ \psi b}^{sr} & \underline{K}_{\sigma\ \psi\psi}^{sr} \end{bmatrix} \tag{20}$$

The residual force and nodal displacement vectors $\underline{R}^s$ and $\Delta \underline{\delta}^r$ respectively are defined as follows

$$\Delta \underline{\delta}^r = \begin{bmatrix} \Delta \underline{\delta}_o^r \\ \Delta \underline{\delta}_b^r \\ \Delta \underline{\delta}_{\psi}^r \end{bmatrix} \qquad \underline{R}^s = \begin{bmatrix} \underline{R}_o^s \\ \underline{R}_b^s \\ \underline{R}_{\psi}^s \end{bmatrix} \tag{21}$$

The tangential stiffness matrix and non-linear stiffness matrices terms of equation (19) and (20) have been defined in [11].

FACETTED SHELL FINITE STRIP ELEMENTS

Local and Global Axes [9]

Each component (plate) forming a box structure or a stiffened plate may have different individual local axes (defined here as x_L, y_L, z_L axes) and it is advantageous to use just one unique global system of axes for the whole structure, such as that shown in figure 1. For finite strip analysis, the *y*-axis will remain the same for all axes systems, i.e. the local *y*-axis is assumed parallel to the global *y*-axis. As an example, a folded plate may have three different local axes and may be as shown in figure 2.

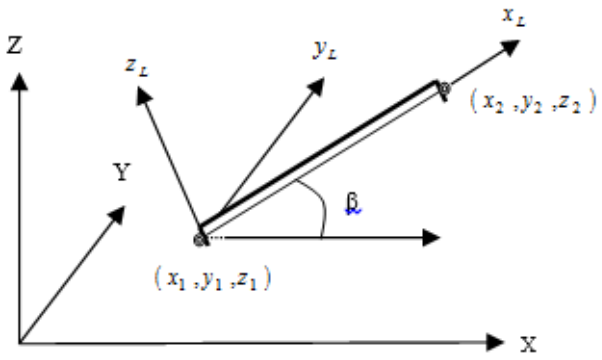

Figure 1. Plate local and global axis

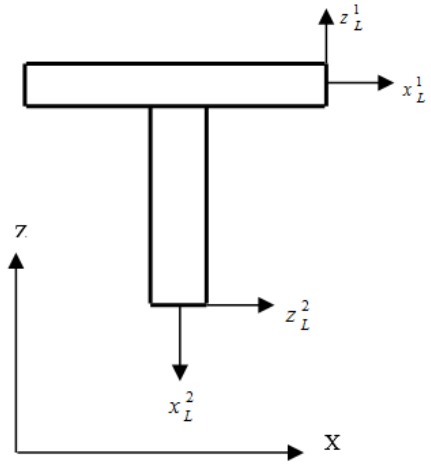

Figure 2. Local and global axes of a folded plate

Local axes for a finite strip element are defined in terms of the two end points of the strip such that:

- The local x axis is from the first end to the second end.
- The local *y*-axis is in the midplane of the strip, and normal to the *x*-axis.
- The local *z*-axis is normal to the $x_L - y_L$ plane (the midplane $z_L = 0$), across the thickness.

If (x_1, y_1, z_1), (x_2, y_2, z_2) are the global coordinates of the two end points of the strip on the $x_L - z_L$ plane, i.e. with $y_1 = y_2 = 0$, then the angle β between the local *x*-axis and the global *x*-axis can be defined, as shown in figure 1, hence

$$\cos\ \beta = \frac{x_2 - x_1}{L},\quad \sin\ \beta = \frac{z_2 - z_1}{L} \qquad (22)$$

where $L = \sqrt{(x_2 - x_1)^2 + (z_2 - z_1)^2}$ (23)

which represents the length of the finite strip in the x_L – direction. Hence, the directional cosines (l_1, m_1, n_1) of the local *x*-axis with respect to the global axes can be defined as follows:

$l_1 = \cos\beta, m_1 = 0, n_1 = \sin\beta$ (24)

and from geometry, the directional cosines, (l_3, m_3, n_3) of the local *z*-axis are:

$l_3 = -\sin\beta, m_3 = 0, n_3 = \cos\beta$ (25)

Also, the directional cosines (l_2, m_2, n_2) of the local *y*-axis are:

$l_2 = 0, m_2 = 1, n_2 = 0$ (26)

Hence, the rotation matrix $\underline{R}$ of the local axes can be defined as the following:

$$\underline{R} = \begin{bmatrix} l_1 & m_1 & n_1 \\ l_2 & m_2 & n_2 \\ l_3 & m_3 & n_3 \end{bmatrix} = \begin{bmatrix} \cos\beta & 0 & \sin\beta \\ 0 & 1 & 0 \\ -\sin\beta & 0 & \cos\beta \end{bmatrix} \quad (27)$$

ROTATION VECTOR [9]

Notice that if $\hat{i}, \hat{j}, \hat{k}$ are unit vectors in the global *x, y, z* directions, and $\hat{i}_L, \hat{j}_L, \hat{k}_L$ are unit vectors in the local x_L, y_L, z_L directions then it can be deduced that:

$$\left.\begin{aligned} \hat{i}_L &= l_1\hat{i} + m_1\hat{j} + n_1\hat{k} \\ \hat{j}_L &= l_2\hat{i} + m_2\hat{j} + n_2\hat{k} \equiv \hat{j} \\ \hat{k}_L &= l_3\hat{i} + m_3\hat{j} + n_3\hat{k} \end{aligned}\right\} \quad (28)$$

which can be written in a matrix form as follows:

$$\begin{bmatrix} \hat{i}_L \\ \hat{j}_L \\ \hat{k}_L \end{bmatrix} = \underline{R}\begin{bmatrix} \hat{i} \\ \hat{j} \\ \hat{k} \end{bmatrix} \quad \begin{bmatrix} \hat{i} \\ \hat{j} \\ \hat{k} \end{bmatrix} = \underline{R}^t \begin{bmatrix} \hat{i}_L \\ \hat{j}_L \\ \hat{k}_L \end{bmatrix} \quad (29)$$

i.e. $\underline{R}^{-1} = \underline{R}^t$

A Cartesian vector $\vec{V}$ can be represented by its local components (v_x^L, v_y^L, v_z^L) or global components (v_x, v_y, v_z), i.e.

$$\vec{V} = v_x^L \hat{i}_L + v_y^L \hat{j}_L + v_z^L \hat{k}_L \equiv v_x \hat{i} + v_y \hat{j} + v_z \hat{k} \qquad (30)$$

which can also be represented in a matrix form as follows

$$V = \begin{bmatrix} v_x^L & v_y^L & v_z^L \end{bmatrix} \begin{bmatrix} \hat{i}_L \\ \hat{j}_L \\ \hat{k}_L \end{bmatrix} = \begin{bmatrix} v_x & v_y & v_z \end{bmatrix} \begin{bmatrix} \hat{i} \\ \hat{j} \\ \hat{k} \end{bmatrix} \equiv \begin{bmatrix} v_x^L & v_y^L & v_z^L \end{bmatrix} \underline{R} \begin{bmatrix} \hat{i} \\ \hat{j} \\ \hat{k} \end{bmatrix} \qquad (31)$$

Hence, it can be deduced that:

$$\begin{bmatrix} v_x \\ v_y \\ v_z \end{bmatrix} = \underline{R}^t \begin{bmatrix} v_x^L \\ v_y^L \\ v_z^L \end{bmatrix} \qquad (32)$$

Similarly it can be proved that:

$$\begin{bmatrix} v_x^L \\ v_y^L \\ v_z^L \end{bmatrix} = \underline{R} \begin{bmatrix} v_x \\ v_y \\ v_z \end{bmatrix} \qquad (33)$$

Degrees of Freedom and Rotation Matrix for Reissner-Type elements

The interpolation equations of Reissner-type element are based upon six degress of freedom per node *i* and per *y* term *r*; u_i^r, v_i^r, w_i^r, $w_{i,x}^r$, $(\psi_x^r)_i$, $(\psi_x^r)_i$, with their directions are as shown in figure 3.

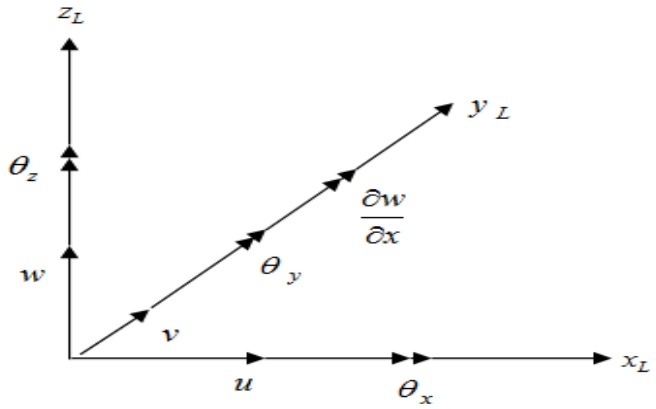

Figure 3. Degrees of freedom for Reissner-type finite strip element

Similarly, for facetted elements additional degrees of freedom $\left(\psi_z^r\right)_i$ is needed with the following considerations:

- For co-planar nodes:

We consider $\left(\psi_z^r\right)_i = 0$ at all y terms, and ψ_x, ψ_y will always be considered in the directions of the local *x*, *y*-axes.i.e. for a co-planar node *j*:

$$\begin{bmatrix} \left(\psi_x^r\right)_j \\ \left(\psi_y^r\right)_j \\ \left(\psi_z^r\right)_j \end{bmatrix}_{Local} = \underline{I} \begin{bmatrix} \left(\psi_x^r\right)_j \\ \left(\psi_y^r\right)_j \\ \left(\psi_z^r\right)_j \end{bmatrix}_{Global}, \left(\psi_z^r\right)_j = 0 \qquad (34)$$

- For node *i* at the intersection of two plates:

The global ψ_z may not be equal to zero and we use the following equation:

$$\begin{bmatrix} \left(\psi_x^r\right)_i \\ \left(\psi_y^r\right)_i \\ \left(\psi_z^r\right)_i \end{bmatrix}_{Local} = \underline{R} \begin{bmatrix} \left(\psi_x^r\right)_i \\ \left(\psi_y^r\right)_i \\ \left(\psi_z^r\right)_i \end{bmatrix}_{Global} \qquad (35)$$

Hence, the rotation, matrix of the *Reissner*-type element at any node *i* and *y* value r can be defined such that:

$$\begin{bmatrix} u_i^r \\ v_i^r \\ w_i^r \\ w_{i,x}^r \\ \left(\psi_x^r\right)_i \\ \left(\psi_y^r\right)_i \\ \left(\psi_z^r\right)_i \end{bmatrix}_{Local} = \underline{R}_i^H \begin{bmatrix} u_i^r \\ v_i^r \\ w_i^r \\ w_{i,x}^r \\ \left(\psi_x^r\right)_i \\ \left(\psi_y^r\right)_i \\ \left(\psi_z^r\right)_i \end{bmatrix}_{Global} \qquad (36)$$

where for a co-planar node *j*:

$$\underline{R}_j^H = \begin{bmatrix} \underline{R} & 0 & \underline{0} \\ 0 & 1 & 0 \\ \underline{0} & 0 & \underline{I} \end{bmatrix} \qquad (37)$$

and for node *i* at the intersection of two plates:

$$\underline{R}_i^H = \begin{bmatrix} \underline{R} & 0 & \underline{0} \\ 0 & 1 & 0 \\ \underline{0} & 0 & \underline{R} \end{bmatrix} \qquad (38)$$

Finally, for all the components of an n-node finite strip element at the *rth y* term or harmonic, we can deduce that:

$$\underset{7n\times 1}{\underline{\delta}^{r}_{Local}} = \underset{7n\times 7n}{\mathfrak{R}} \; \underset{7n\times 1}{\underline{\delta}^{r}_{Global}} \qquad (39)$$

where $\mathfrak{R}$ is the element rotation matrix defined as follows:

$$\mathfrak{R} = \left| \underline{R}_1^{H} \quad \underline{R}_2^{H} \cdots \quad \underline{R}_i^{H} \cdots \quad \underline{R}_n^{H} \right| \qquad (40)$$

An additional boundary condition should be implemented for every co-planar node *j*:

$$\left(\psi_z^{r}\right)_j = 0, \text{ for } r = 1,2,3, \ldots, m \qquad (41)$$

From the derivations of the stiffness matrices in the previous chapters, it can be deduced that:

$$\underline{K}_{Global}^{sr} = \mathfrak{R}^{t} \; \underline{K}_{Local}^{sr} \; \mathfrak{R} \qquad (42)$$

and

$$\underline{K}_{\sigma\, Global}^{sr} = \mathfrak{R}^{t} \; \underline{K}_{\sigma\, Local}^{sr} \; \mathfrak{R} \qquad (43)$$

IV NUMERICAL EXAMPLES

The first paragraph under each heading or subheading should be flush left, and subsequent paragraphs should have a five-space indentation. A colon is inserted before an equation is presented, but there is no punctuation following the equation. All equations are numbered and referred to in the text solely by a number enclosed in a round bracket (i.e., (3) reads as "equation 3"). Ensure that any miscellaneous numbering system you use in your paper cannot be confused with a reference [4] or an equation (3) designation.

An analysis of a stiffened plate is considered in this case in order to demonstrate the ability of the newly derived finite strips methods to deal with folded plates problems. In this test case, a simple stiffened plate, which is shown schematically in figure 4 is considered, where

Length in x-direction L = 2 m,
Width in y-direction, B =1 m,
Height of the stiffener in z-direction S = 0.5 m.

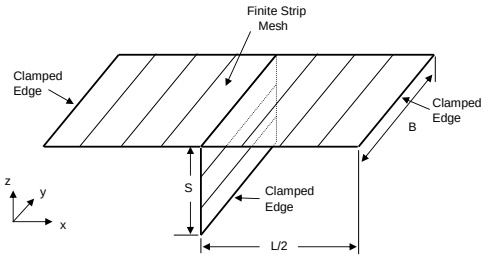

Figure 4. Geometry and boundary conditions of Stiffened plate.

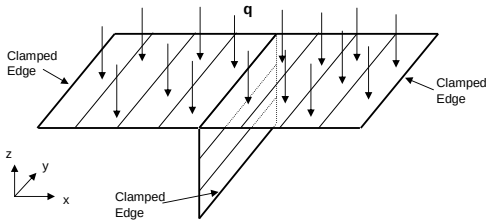

Figure 5. Stiffened plate under uniform distributed load.

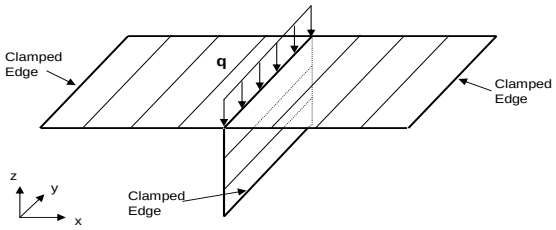

Figure 6. Stiffened plate under uniform line loading.

The plates consist of 12-ply ($[-45/0/45]_{2S}$) Carbon-Epoxy composite whose material properties are given in Table 1.

TABLE I. Mechanical Properties of the stiffened plates

Parameter	Value
Longitudinal Modulus E_{11} [GPa]	12.61
Transverse Modulus E_{22} [GPa]	12.61
Shear Modulus in x-y plane G_{12} [GPa]	2.15
Shear Modulus in y-z plane G_{23} [GPa]	2.15
Shear Modulus in z-x plane G_{31} [GPa]	2.15
Major Poisson's Ratio v_{12}	0.29
Thickness of each layer [mm]	0.6

The stiffened plate has been tested by using two types of load cases:

1) Case with distributed loading (figure 5) on the upper surface, along –z –direction (thickness), with intensity of 2.0×10^5 N/m^2.
2) Case with out-of-plane line loading (figure 6), with load intensity of 2.0×10^6 N/m.

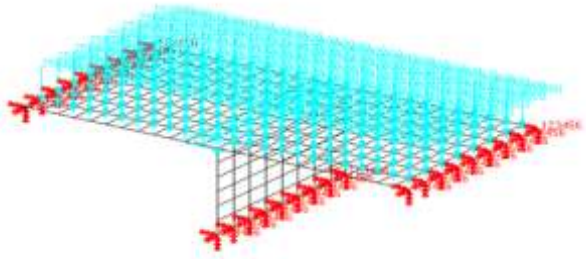

Figure 7. ABAQUS stiffened plate finite element mesh and boundary conditions under uniform distributed load.

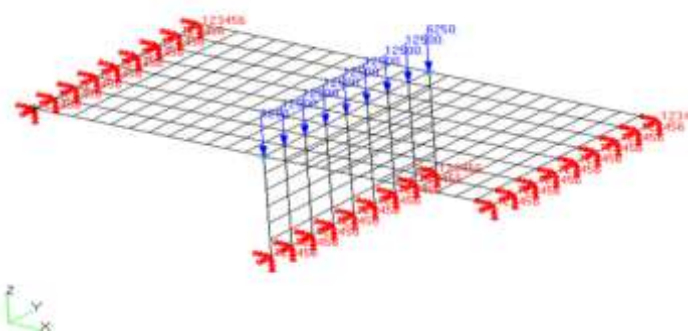

Figure 8. ABAQUS stiffened plate finite element mesh and boundary conditions under uniform line loading.

For validation purposes, 11 finite strip elements based on Reissner (Hermitian) type of element were used to model the plate whereas 6 elements were used for the stiffener for both test cases. On the other hand, finite element mesh and boundary conditions were modelled using the ABAQUS S4 shell element [11]. Figures 7 and 8 show the mesh and boundary conditions for cases with distributed loading and line loading respectively.

The results for the load increment (reaction force in z-direction measured at the bottom of the stiffener) versus the out-of-plane deflections, *w* at mid-point of the stiffened plate, i.e. at (L/2, B/2) were compared with the results obtained from ABAQUS for both cases. As can be seen in figures 9 and 10 excellent agreement between the finite strip and finite element results has been achieved.

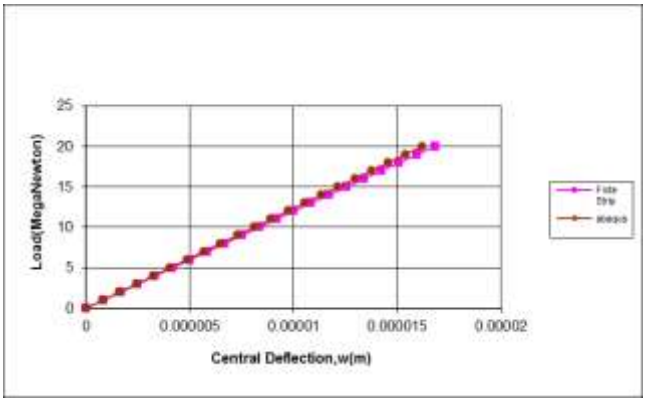

Figure 9. Load vs central deflection of stiffened plate under uniform distributed.

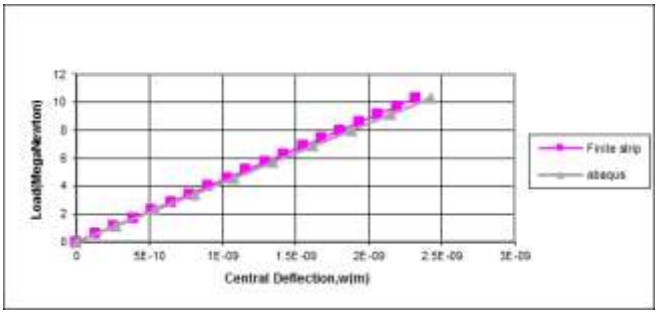

Figure 10. Load vs central deflection of stiffened plate under uniform line loading.

V CONCLUSION

The work presented in this research contributes to the development of a finite strip method capable of performing a non-linear static analysis of composite laminated plates based on a higher order finite strip element, which may be used in the design and analysis of prismatic shape composite laminated structures. Validation of the developed finite strip package has been successfully carried out by comparing the results with the finite element analysis using ABAQUS. Good agreement with the finite element results (ABAQUS) were observed

from previous test cases, confirming the accuracy and reliability of the new derivations and the programming package. A reduction in the modelling effort and time can be achieved as a result of only one-dimensional mesh required to model facetted shells by using the package built-in mesh generator as compared to the conventional 2-dimensional finite element mesh.

REFERENCES

[1]. Zahari R., Mustapha F,Majid, D.L.A., Shakrine A., Sultan T.H. Geometric non-linear analysis of composite laminated plates using higher order finite strip element. *Applied Mechanics and Materials, 226*, 2012, 165-171.

[2]. Cheung, Y.K. The finite strip method in the analysis of elastic plates with two opposite simply supported ends. *Proc. Inst. Civil Engng, 40*, 1968, 1-7.

[3]. Kermanidis, T.B. & Labeas, G.N. Static and stability analysis of composite plates by a semi-analytical method. *Computers & Structures*, *57*, 1995, 673-679.

[4]. Wang, W.J., Tseng, Y.P. & Lin, K.J. Stability of laminated plates using finite strip method based on higher-order plate theory. *Composite Structures*, *34*, 1996, 65-76.

[5]. Akhras, G., Cheung, M.S. & Li, W. Geometrically nonlinear finite strip analysis of laminated composite plates. *Composites Part B, 29B*, 1998, 489-495.

[6]. Loughlan, J. The influence of mechanical couplings on the compressive stability of anti-symmetric angle-ply laminates. *Composite Structures,57*, 2002, 473-482.

[7]. Reissner, E. The effect of transverse shear deformation on the bending of elastic plates. *Journal of Applied Mechanics*, *12*, 1945, 69-76.

[8]. Mindlin, R.D. Influence of rotary inertia and shear in flexural motions of isotropic elastic plates. *Journal of Applied Mechanics*, *18*, 1951,31-38.

[9]. Zahari, R. & El-Zafrany, A) Progressive Failure Analysis of Composite Laminated Stiffened Plates using the Finite Strip Method. *Composite Structures*, *87*, 2009, 63-70.

[10]. Zienkiewicz, O.C. & Taylor, R.L. *The finite element method. 5th edition*, (Butterworth & Heinemann, Oxford, 2000).

[11]. Zahari.R. *Progressive Damage Analysis of Composite Layered plates using the Finite Strip Methods*. Doctoral diss., Thesis, Cranfield University, United Kingdom, 2005.

[12]. ABAQUS. *ABAQUS User's manual, Vol. 1-3, Version 6.8.* (Pawtucket, RI:Hibbitt, Karlsson & Sorensen, 2008).

Rizal Zahari." Development of Composite Laminated Faceted Shells Using a Higher Order Finite Strip Element." The International Journal of Engineering and Science (IJES) 7.5 (2018): 35-46